Restraining force and moment of reinforced concrete beam-column under a sustained long-term temperature crossfall

T.Ikoma & N.Tanaka
Institute of Technology, Shimizu Construction Co. Ltd, Tokyo, Japan

1. INTRODUCTION

It has been generally considered that the design bending moment for a nuclear reactor building, especially for a reinforced concrete (RC) containment vessel, is mostly dominated by the thermal load. According to the thermal stress experiment with the thermal load applied for a short time, the ratio of the RC flexural rigidity at the level of long-term allowable stress of reinforcements to elastic flexural rigidity ranges from 1/3 to 1/2[1].

It is also considered that the creep effect, one of the characteristics of concrete, becomes more significant as the thermal load acts on RC for a long time. There have been few experiments however aiming at such an effect, besides they were ones which aimed only the bending moment.

Noting these facts, in order to clarify not only the bending moment by the thermal load but also the behavior of the axial force, the decreasing trend of bending moments and axial forces caused by the cracks and creeps have been experimentally confirmed by applying constant thermal loads for 60 days to the beam-column structures having various reinforcement ratios in RC, and by generating actual thermal stresses. It is not possible, however, to directly find the axial force and bending moment as an internal force caused by the thermal load because of the testing method, thus the restraining axial force and restraining bending moment as an external force equivalent to the above values are detected and shown in this report. The effect of ambient temperature and deformed loadcells, however, which affect the restraining axial force and bending moment, is not considered in this report.

2. OUTLINE OF EXPERIMENT

2.1 Shape and size of test pieces

Three kinds of test pieces were used ; A model, a T-shape consisting of a beam and a column, and B and C models, both of which were I-shaped and consisted of just a column. All of the test pieces except B model had a fixing portion at each member end not only for fixing the test piece but also for restraining thermal deformation.

These test pieces are detailed in Figs. 1 to 3. In these figures, the portions to be tested are 3,000 mm long members having a uniform cross section.

As for testing parameter during the experiment, the relative differences in reinforcement ratios between beam and column of only A model are taken into consideration. Concretely speaking, keeping the reinforcement ratio of the

column portion constant, three types of reinforcement ratios were employed, i.e., compared with the reinforcement ratios in the column, those in the beam portion were set larger, equal and smaller in values (actually P_t=1.2%, 0.7%, 0.4%).

2.2 Concrete and reinforcements used

Normal concrete was used to make the test pieces. Approximately 50 day safter concrete-casting, the test was started. Unexpectedly, cracks had occurred in test pieces of A-2 and C-1 when they were set to the concrete restraining block. On test piece A-2 in particular, the crack generated was deep enough to penetrate the section around the base of its column.

2.3 Properties of test pieces

The properties of the test pieces used in the experiment are listed in Table 1. As stated above, it is quite clear that the strengths of concrete used for test pieces A-2 and C-1 were relatively low (both at the test start and at the test finish).

2.4 Heating procedure of test pieces

The heated portions were limited to just the columns of the test pieces A, B and C. Heat was applied to both sides of the columns' shorter face by using hot water heated at 80℃ for one side and cold water cooled at 20℃ for the other side while keeping temperature of the above waters constant and circulating such water in a rubber bag. The test pieces were heated by bringing these rubber bags directly into contact with the test pieces.

The concrete surface of all the test pieces was not sealed, but all surfaces other than the contact surface of the rubber bag were covered with an insulating material so as to minimize the influence of atmospheric temperature.

2.5 Procedure for restraining test pieces

The test pieces were restrained in the following procedure. First, by fixing the concrete blocks to the floor surface with PC steel bars, and then by directly fixing the test pieces to the concrete blocks with PC steel bars. More specifically, each beam end of A model was directly anchored, and just the column top of B model and C model was anchored by using PC steel bars respectively. In order to increase the restraining effect between each test piece end and the concrete blocks, plaster was filled into the gap.

Next, at the base of the column of A model and C model, which were the test pieces for restraining the thermal deformation, H-shape steel of 500 mm × 500 mm×2400 mm was placed, through which one loadcell (L_1) to detect the "restraining force" was placed on the high temperature side and three loadcells (L_2, L_3, L_4) were placed on the low temperature side (L_3 was placed normal to the column axis). Thus four loadcells were used.

As for B model, the restraint of the column base was removed so as to generate thermal deformation freely. The general configuration and shape of this testing set-up is illustrated in Fig. 4.

2.6 Measurement items

Items measured in this experiment were as follows ;

(1) Restraining forces (L_1 to L_4) when thermal deformation were restrained
(2) Temperatures inside the beam and column
(3) Displacement of beam and column (normal to each member's axis)
(4) Cracks on the test pieces

In addition to the above items, the following were also measured ;

(5) Temperatures of heating media (hot water, cold water)
(6) Temperatures in the laboratory

3. EXPERIMENTAL RESULTS

3.1 Definition of terms related to temperature

In order to clarify the temperature conditions inside the test pieces when evaluating the test results, two terms which may different in effect mechanically from each other should be defined.

One is the quantity concerning the restraining force, which is called average temperature rise (ΔT_d), the other is the quantity concerning the restraining bending moment, which is called the equivalent temperature gradient ($\Delta T_g/D$, where D is a total depth of column).

ΔT_d and $\Delta T_g/D$ can be defined through the temperature distribution converted to a straight line (assume T_h=highest temperature, T_l=lowest temperature) so that ΔT_d and $\Delta T_g/D$ can be a force system equivalent to an axial force and a bending moment as an internal force induced when the thermal strain is restrained, where the thermal strain is considered to be generated by an actual temperature distribution of a column section at a given time (See Fig. 5). Thus these two quantities can be defined as follows :

$$\Delta T_d \equiv (T_h + T_l)/2 - T_0 \quad (1)$$

$$\Delta T_g/D \equiv (T_h - T_l)/D \quad (2)$$

where T_0 is generally called a stress free temperature, which corresponds to strainless conditions of the test pieces before heating.

3.2 Temperature of heating media and air in the laboratory

Figures 6 shows the temperatures of hot and cold water as heating media and temperature changes in the laboratory for B model. In this figure the portions where the temperature of cold water deviates from the temperature set correspond to the time of failure in the temperature controller.

3.3 Transition of restraining force

The results of the restraining force, defined as the indicated value of the four loadcells above, are shown below except for L_3. As for L_3, measurement could not be done even with the loadcell of full scale of 2 tons and an accuracy of 1/5000.

3.4 Curvature at free thermal deformation

Figure 7 shows $\Delta T_g/D$ and free thermal deformation curvature by time of B model. In this figure, three types of lines representing curvature (thick full line, fine full line and dotted line) show the curvature and its average value (dotted line) obtained from the displacement at two any point. It is clear in this figure that the curvature increases rapidly as $\Delta T_g/D$ increases, reaching the maximum value 1.07×10^{-5}/cm. Thereafter, contrary to $\Delta T_g/D$ being constant not decreased, the curvature continues decreasing gradually and becomes close to a constant value at about 40 days after the heating of the test piece was started.

It is also clear that this curvature responds very rapidly to the disturbance of temperature distribution (portion where $\Delta T_g/D$ changes abruptly in the figure). The change of a thermal expansion coefficient by time was obtained based on the following equation for the curvature and equivalent temperature gradient.

$$\frac{1}{r} = \alpha \ (\Delta T_g/D) \quad (3)$$

This thermal expansion coefficient, for reference, can be expressed as the following experimental equation.

$$\alpha = a \cdot e^{-k(t-t_0)} + b \quad (t > t_0) \tag{4}$$

where,

$$\left.\begin{array}{lll} a & = & 0.416\times10^{-5} \ (1/℃) \\ b & = & 0.495\times10^{-5} \ (1/℃) \\ k & = & 0.0597 \quad\quad (1/day) \\ t_0 & = & 0.5 \quad\quad\ (day) \end{array}\right\} \tag{5}$$

3.5 Displacement of test pieces

Figures 8 to 10 show the maximum displacement modes of each test piece. The amount of free thermal deformation of B model, whose column base was not restrained, should be noted.

4. CONSIDERATION OF TEST RESULTS

4.1 Restraining axial force and restraining moment

Figure 11 shows the changes by time of the restraining axial force (F_r) and restraining moment (M_r) measured on A-3, C-2 models, where F_r and M_r are defined as follows :

$$F_r \equiv L_1 + (L_2 - L_4) \tag{6}$$

$$M_r \equiv (L_1 - (L_2 - L_4))\,l/2 \tag{7}$$

where l is the distance between the supporting points of L_1 and $(L_2 - L_4)$. In the figure, the reason the sways of the restraining axial force F_r are much greater than those of the restraining moment is why the sways of the restraining force L_1 and $(L_2 - L_4)$ due to daily atmospheric temperature were set off to each other, as is clear from the Eq. (7) defining M_r. From this figure, it should also be noted that F_r in terms of time past decreases to 1/5 of the maximum value in about 30 days.

Figure 12 was obtained in the form of ratio of F_r and M_r in the previous figure to elasticity calculation values defined by the following formulas.

- Elastic thermal axial force :

$$F_T \equiv (\alpha \cdot \Delta T_d)\, E_c \cdot A_g \tag{8}$$

- Elastic thermal bending moment :

$$M_T \equiv (\alpha \cdot \Delta T_g/D)\, E_c \cdot I_g \tag{9}$$

where α is a linear expansion coefficient as RC member (0.91×10^{-5}/℃) corresponding to the maximum value of the free thermal deformation curvature of B model (See Fig. 7). E, A and I show Young's modulus, the sectional area of the tested portion and the geometrical moment of inertia before the test pieces were heated, respectively. Letters c and s represent only the concrete and reinforcement respectively, and the amount with letter g can be defined as follows :

$$A_g \equiv A_c + n \cdot A_s \tag{10}$$

$$I_g \equiv I_c + n \cdot I_s \tag{11}$$

where n is Young's modulus ratio (E_s/E_c) and 15 is employed as this ratio herein.

From this figure, it is clear that the nondimensional restraining moment (M_r/M_T) reaches 0.92 (for C-2 model) and 0.78 (for A-3 model) in each maximum value, but these values gradually decrease as the time passes to 0.2 approximately, after about one month from after the start of heating. It is also evident from this figure that the maximum values of the nondimensional restraining axial force (F_r/F_T), on the other hand, reach 0.33 (for C-2 model) and 0.16 (for A-3 model) and the restaining axial force decreases further continuously, thus finally approaching zero.

4.2 F_r and M_r due to member rigidity

As for the parameters in this experiment, the reinforcement ratio was employed. In other words, it can be said that this has the same meaning as noting the difference in an initial elastic rigidity of a column member and a beam member. Furthermore, it can also be said that this means the same as noting the difference in restraining effect on the column member when only its member is heated and the thermal deformation is ready to occur. From these view points, consideration is given below to a restraining axial force or a restraining moment produced by the difference in rigidity of each member of a beam and column.

Figure 13 shows the restraining axial forces (F_r) corresponding to the ratio of elastic axial rigidity, and Fig. 14 shows the restraining moment (M_r) corresponding to the ratio of elastic flexural rigidity. In both figures, the days past after the start of heating the test pieces (0.5, 10 and 30 days) are chosen as parameter. Infinity (∞) on the abscissa refers to C model, which can be actually regarded as infinity for the beam's rigidity compared with the column's rigidity (especially C-2 model in which cracks did not occur when the test piece was set).

From these figures, it is clear that on the restraining axial force and restraining moment shown in dimensionless form, the restraining moment reaches about 3 to 5 times the restraining axial force about after half a day when these values reach maximum, and thereafter this tendency remains almost unchanged even as the heating time passes. This means that internal axial force equivalent to thermal stress induced in a column portion of a test piece decreases to 1/3 to 1/5 times the internal bending moment equivalent to thermal stress through whole heating period.

Moreover, it is a matter of course from these figures that the lower a beam's elastic rigidity, the greater the decrease in the restraining effect against thermal deformation of a column member. As a result, it is also clear that the axial force and bending moment required to restrain decrease as well.

5. CONCLUSION

From these figures, the following can be concluded :

(1) In view of the nondimensional restraining axial force or nondimensional restraining moment, the reduction rate of a restraining axial force is greater than that of a restraining moment. In particular, the reduction rate just after the start of heating, a restraining axial force is 3 to 5 times larger than that of a restraining moment.

(2) As for an elastic rigidity ratio due to the difference in reinforcement ratio of beam to column, the less the elastic rigidity ratio in both the restraining axial force and restraining moment, the larger the reduction becomes. This tendency continues even as days pass after the start of heating.

(3) Both the restraining axial force and restraining moment gradually

decrease as time passes after the start of heating, and approach a constant value. In addition, the restraining axial force decreased to 1/5 of the maximum value in half a month to a month, depending on the degree of restraint.

REFERENCE

(1) K. Irino and T. Ikoma et al., : "Fundamental Experiments on Thermal Stress of Heated Reinforced Concrete Beams (Part Ⅰ～Ⅲ)", Proc. 1981 Ann. Meet. Arch. Inst. Jap., 1981.

Table 1 Mechanical properties of test pieces

Test pieces		Reinforcement Number and Diameter		Reinforcement ratio (one side) (%)	Restraint	Concrete strength in the air (kgf/cm²) At the start (normal temp.) Compressive strength	At the start (normal temp.) Young's modulus	At the end (normal temp.) Compressive strength	At the end (normal temp.) Young's modulus	At the end (80°C) Compressive strength	At the end (80°C) Young's modulus
A model	A-1	B	4D19	0.7	Yes	241.2	2.33×10^5	243.5	2.27×10^5	244.3	2.24×10^5
		C	4D19	0.7							
	A-2*	B	4D13	0.4		159.5	1.86×10^5	152.0	1.72×10^5	151.4	1.27×10^5
		C	4D19	0.7							
	A-3	B	4D25	1.2		229.6	1.81×10^5	260.2	2.25×10^5	234.3	1.80×10^5
		C	4D19	0.7							
B model	B	C	4D19	0.7	No	241.2	2.33×10^5	243.5	2.27×10^5	244.3	2.24×10^5
C model	C-1*				Yes	159.5	1.86×10^5	152.0	1.72×10^5	151.4	1.27×10^5
	C-2					229.6	1.81×10^5	260.2	2.25×10^5	234.3	1.80×10^5

B: Beam, C: Column (1 kgf=9.8N)
(*): Test piece in which cracks occurred before testing

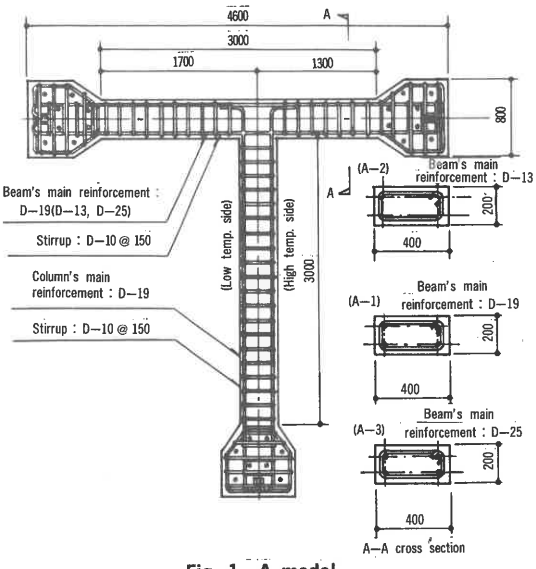

Fig. 1 A model

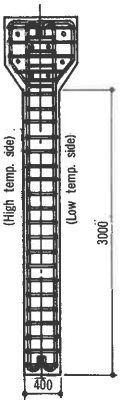

Fig. 2 B model

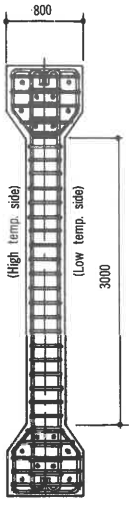

Fig. 3 C model

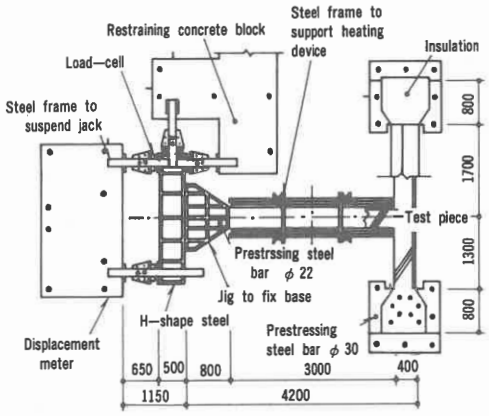

Fig. 4 Test set-up

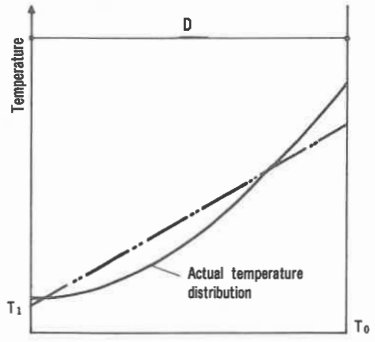

Fig. 5 Definition of temp.

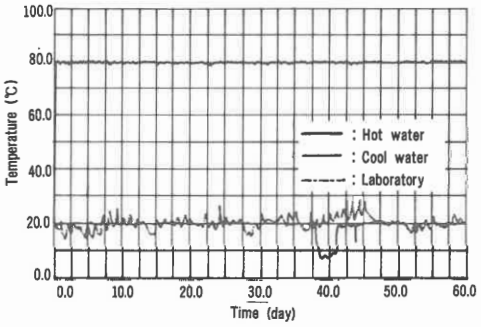

Fig. 6 Ambient temp. of B model

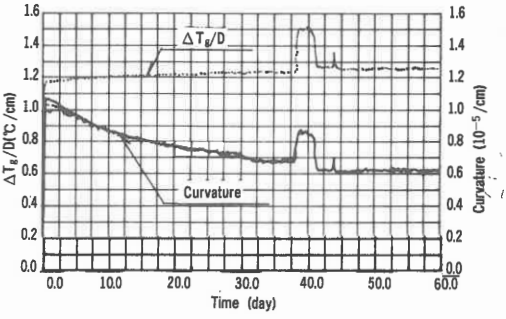

Fig. 7 Curvature of B model

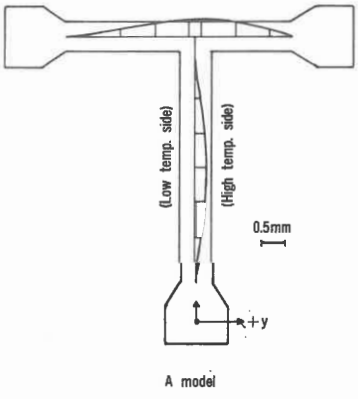

Fig. 8 Maximum displacement mode

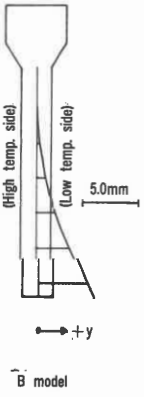

Fig. 9

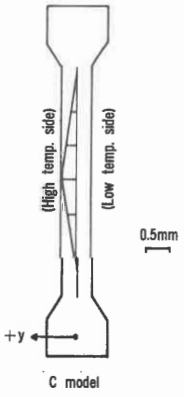

Fig. 10

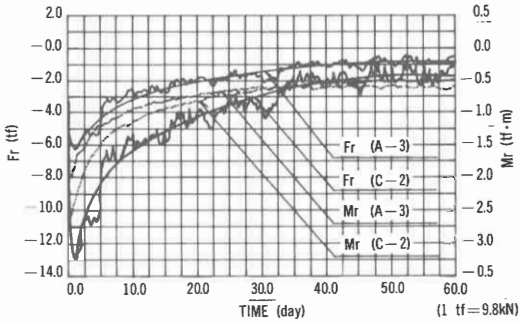

Fig. 11 Restraining axial force and moment

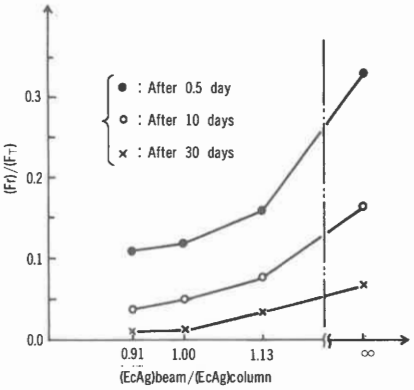

Fig. 13 Fr and axial rigidity

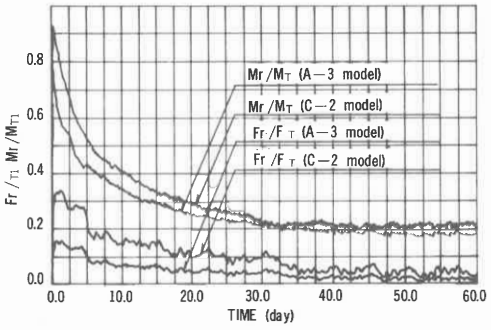

Fig. 12 Nondimensional Fr and Mr

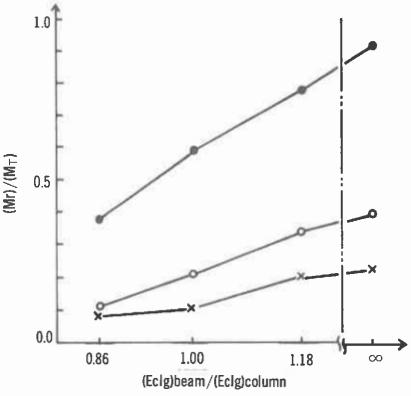

Fig. 14 Mr and flexural rigidity